A study of perpendicular Ag hyperfine fields induced at the interface in Fe/Ag multilayer systems

T. Phalet,[1] M. J. Prandolini,[1,*] W. D. Brewer,[2] P. Schuurmans,[1,†] N. Severijns,[1] B. G. Turrell,[3] B. Vereecke,[1] and S. Versyck[1]

[1]*Instituut voor Kern- en Stralingsfysica, Katholieke Universiteit Leuven, B-3001 Leuven, Belgium*

[2]*Institut für Experimentalphysik (WE1), Freie Universität Berlin, 14195 Berlin, Germany*

[3]*Department of Physics, University of British Columbia, Vancouver, British Cloumbia, Canada V6T 2A6*

(Received 21 September 2004; revised manuscript received 11 January 2005; published 29 April 2005)

In a series of experiments the hyperfine fields of Ag at the interface with Fe were measured in Fe/Ag multilayers using the low temperature nuclear orientation technique. The thickness of the Fe layers was chosen so that the in-plane shape anisotropy would dominate over the perpendicular surface anisotropy. However, for multilayers with a well ordered multilayer structure as measured by x-ray diffraction, the Ag magnetic hyperfine fields were found to be nearly perpendicular to the layer plane. The out-of-plane magnetic structure of the induced Ag magnetic moments has been also supported by vibrating sample magnetometry measurements on the same samples. In addition, the magnitude of the induced Ag hyperfine fields are significantly reduced by roughness. Calculations using WIEN97 confirm that the Ag hyperfine fields are strongly affected by the number of nearest Fe neighbors and their distance.

DOI: 10.1103/PhysRevB.71.144431 PACS number(s): 75.70.−i, 31.30.Gs

I. INTRODUCTION

Thin two-dimensional multilayer systems are finding an increasing use in industry because they allow the engineering of materials with new magnetic properties. One important property afforded by the two-dimensional interface between a magnetic and a nonmagnetic surface is enhanced perpendicular magnetic anisotropy. Presently, almost all magnetic recording of digital data uses conventional longitudinal (in-plane) magnetic material. One method in order to achieve ultrahigh-density magnetic recording is the use of a medium which is magnetized perpendicular to the plane.[1]

It was first recognized by Néel[2] that the perpendicular magnetic anisotropy (K_s), induced by symmetry breaking at a surface or an interface, can be quite different from the bulk anisotropy. Since this anisotropy is of short range and restricted to the interface, the anisotropy energy scales inversely with the magnetic film thickness d. Another important factor influencing the total magnetic anisotropy is long range demagnetization fields (shape anisotropy). For single magnetic films, demagnetization fields normally force the magnetization to lie in the plane and is independent of the film thickness except in the ultrathin film limit.[3] The demagnetization energy density can be written as $K_v = \mu_0 M_s^2/2$, where M_s is the saturation magnetization. In the design of systems with perpendicular anisotropy, the ratio of the perpendicular to the shape anisotropy, $(2K_s/d)/K_v$, called the Q factor,[4] is a useful parameter. This quantity can be most easily adjusted by changes in the film thickness. Systems with $Q > 1$ are dominated by perpendicular anisotropy.

In single Ag(001)/Fe(001)/Ag(001) films the critical thickness (i.e., $Q=1$), where Fe changes from having an out-of-plane to an in-plane magnetization as the Fe thickness increases, has been measured to be 5 ML, where $K_v = 1.86 \times 10^6$ J/m^3 and $K_s = 0.64$ mJ/m^2.[5] In addition to changes in ferromagnetic thickness, the surface anisotropy is also strongly influenced by roughness and interface strain due to lattice mismatch. In general, roughness has been shown to decrease the surface anisotropy.[6] In particular, a film Ag/Fe(3.5 ML)/Ag grown on a [001] surface of an Fe whisker (with single atomic steps spaced ~ 1 μm apart) was shown to have greatly improved perpendicular anisotropy compared to rougher samples.[7] However, on an ordered vicinally cut stepped surface the perpendicular anisotropy for the film Ag/Fe/vacuum has been observed to increase, depending quadratically on the step density. This was demonstrated on a 6° vicinally cut Ag(001) substrate where the critical thickness was found to slightly increase to 6.5 ML, compared to 5.5 ML grown on flat Ag(001).[8]

A further parameter can be introduced by forming a multilayer structure, consisting of N magnetic/nonmagnetic bilayers. It has been shown that a magnetization reorientation can be induced in Co/Au multilayers by increasing N, for multilayers with a dominant in-plane anisotropy, i.e., with Q factors of 0.8 and 0.64.[9] It was observed that for such Co/Au multilayers, the magnetization lies in the plane for $N=1$ and 2, however, it reorientates to form a stable magnetic structure consisting of out-of-plane domains (i.e., striper domains) for $N=30$ and 31. The magnetization reorientation was attributed to a reduction in the demagnetization energy originating from the formation of an out-of-plane stripe domain structure.[10]

We have chosen to study the magnetic structure of Fe/Ag(001) multilayers, with Q factors ranging from 0.8 down to 0.28. Multilayers in this range should be strongly magnetized in the plane. Fe/Ag(001) multilayers are an ideal system because there is a small lattice mismatch between the two elements (0.8%), and Fe and Ag are immiscible. Thus making it possible to make multilayers with high structural quality.

Most conventional experimental techniques to probe magnetic properties measure the magnetism of the Fe in the mul-

tilayers. Previous work on the Fe layers in Fe/Ag multilayers include magneto-optic Kerr effect measurements (MOKE),[11,12] scanning electron microscopy with polarized analysis,[13] Mössbauer spectroscopy,[14,15] and ferromagnetic resonance (FMR).[16] These measurements showed the presence of oscillatory interlayer exchange coupling of the Fe layers in Fe/Ag systems. Only a few techniques allow probing of the magnetism in the Ag layers, which is induced by the presence of the magnetic Fe layers. Previous work on the Ag layers was performed using perturbed angular correlations (PAC).[17] In the present work, the magnetic hyperfine fields in the Ag spacers were measured using low temperature nuclear orientation (LTNO).

The LTNO technique is sensitive to the average *magnitude and alignment* ($\langle I_z^2 \rangle$ and higher even orders) of the nuclear spins of the radioactive probe nuclei. Previous theoretical,[18] and experimental[17] hyperfine interaction studies on the Fe/Ag interface have shown that large Ag spin perturbations (hyperfine fields $\geqslant 3$ T), are restricted to the first Ag layer in direct contact with the Fe surface. The large hyperfine fields experienced by the interface Ag nuclei result from the induced valence polarization of the Ag atoms, through hybridization of the Ag *s* electrons with the polarized *d* electrons of the nearest Fe neighbors.[19] The degree of hybridization, and thus the strength of the hyperfine field, is strongly dependent on the Ag-Fe distance. The LTNO technique effectively measures the magnitude and directional alignment of the Ag probe atoms in direct contact with the Fe surface since only hyperfine fields of the order of 3 T or more contribute to the signal when the sample is at temperatures around 6 mK. Therefore, the great advantage of the LTNO method is that the magnetic properties of the Fe/Ag(001) interface can be investigated giving unique additional information without introducing a foreign probe.[18,20,21]

The aim of these investigations is to measure the induced Ag hyperfine field at magnetic saturation for all the measured multilayers. This hyperfine field should be a highly sensitive parameter for the interface structure and quality. These results are correlated with multilayer roughness measurements using x-ray diffraction (XRD). In addition, *ab initio* calculations are performed to explore the Ag hyperfine field at ideal Fe/Ag interfaces, including the dependence of the Ag hyperfine field to the number of nearest Fe neighbors. Second, the average alignment of the induced magnetic Ag hyperfine fields at the Fe/Ag interface for multilayers with low Q is measured by LTNO. The degree of out-of-plane canting in low applied fields is compared with the roughness of the multilayers measured by XRD. Finally, these measurements are complimented by magnetization studies using vibrating sample magnetometry (VSM). In contrast to LTNO, which is sensitive to the magnetization at the interface of a magnetic layer, the VSM technique averages over the entire Fe magnetization of the multilayer.

II. PREPARATION OF THE Fe/Ag MULTILAYERS

A. Growth of the multilayers

The bcc Fe lattice (1 ML = 1.433 Å) closely matches the lattice of fcc Ag (1 ML = 2.043 Å) after a rotation by 45° around the normal to the surface. The resulting in-plane lattice mismatch is only 0.8%. In addition, the elements Fe and Ag are immiscible, which assures that the interdiffusion at the interfaces is low. It should thus be possible to make high quality Fe/Ag superlattices. However, too many lattice steps can disturb the crystalline quality within the layers, since the out-of-plane lattice mismatch is as high as 42.5%.

The Fe/Ag multilayers were grown on a MgO[001] substrate. First, the substrate was annealed for 1 h at 600 °C under a pressure below 5×10^{-7} Torr. Then the substrate was cooled to room temperature and introduced into a Riber molecular beam epitaxy (MBE) system via a UHV transport system. The Fe/Ag multilayers were prepared under a vacuum of 3×10^{-10} Torr during growth.

Since Fe/Ag multilayers grown immediately on to the MgO substrate do not have a good multilayer structure,[22] a 100 Å thick seed layer of Fe(001) was first grown epitaxially on the substrate at a temperature of 175 °C. On this seed layer, the actual multilayer structure was grown at room temperature, using an electron gun to evaporate the Fe at a speed of 0.3 ML/s, while the Ag was evaporated from a Knudsen cell at 990 °C with a speed of 0.5 ML/s. The bilayer structure was repeated 20 times. To protect the system, a final capping layer of 500 Å Fe(001) was added to the multilayer.

The structure of the multilayer part of the samples can be written as: $[\mathrm{Ag}(x\ \mathrm{ML})/\mathrm{Fe}(y\ \mathrm{ML})]_{20}$, with the thickness of the layers given in monolayers. The multilayers used in this work had (x,y) values of (2,10), (3,9), (3,17), (6,9), and (4,6), thus with estimated Q factors of 0.53, 0.48, 0.28, 0.48, and 0.80, using $K_s = 0.64\ \mathrm{mJ/m^2}$.[5] All multilayers except the (3,9) were cut into two parts of 10×5 mm each, using a diamond wire saw. The (3,9) system was made larger, and it was divided in three parts: two with an Fe capping layer, and one without capping. This last multilayer will be indicated as: $(3,9)^{\mathrm{no\ cap}}$.

B. Irradiation of the multilayers

In order to investigate the Ag in the multilayers with LTNO, the samples were activated by thermal neutron irradiation at the BER-II reactor of the Hahn-Meitner Institute in Berlin. The neutron flux during irradiation was $\Phi = 10^{13}\ n/(\mathrm{cm^2\ s})$ and the temperature never exceeded 80 °C. During this irradiation, ^{109}Ag nuclei captured a neutron and transformed into the radioactive isomeric state $^{110}\mathrm{Ag}^m$, which has a half-life of 249.7 days and decays to ^{110}Cd. One of the two pieces of each multilayer was irradiated for 10 days, while the other was irradiated for 35 days.

Before and after irradiation, and again before the LTNO measurements, the quality of the multilayers was checked using XRD. This showed that a 10 day activation does not induce any change in the XRD spectra, whereas a 35 day irradiation caused detectable damage. A good example is the (6,9) system: the roughness (see Sec. III) of the Ag layers after growth (and also after a 10 day irradiation) was found to be 0.50 ML, but after 35 days of irradiation, the roughness had increased to 0.81 ML, an increase of 62%. However, just before the LTNO measurement that was carried out three months later, the XRD spectra of the sample showed a

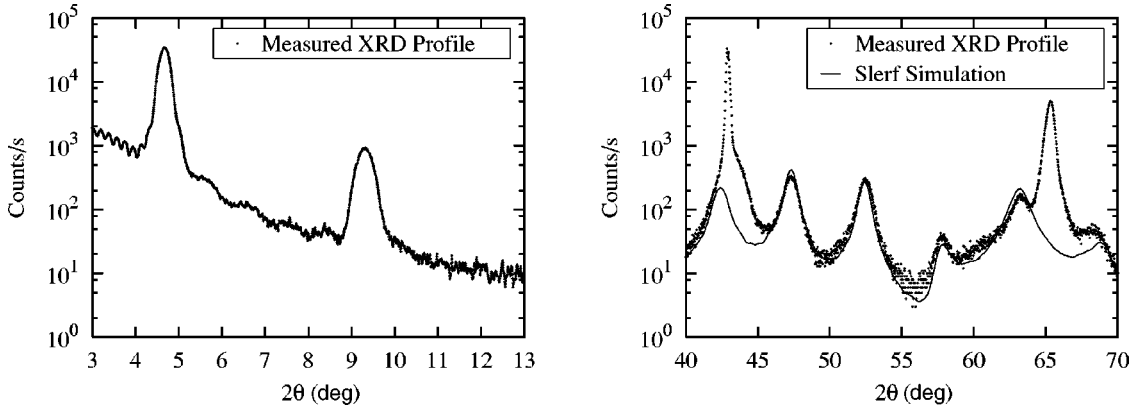

FIG. 1. The low angle and high angle XRD spectra for the (3,9) multilayer. For the high angle spectrum, the SLERF simulation is also shown. Note that two peaks are not simulated. The peak at $2\theta = 42°54'$ is a MgO peak from the substrate, while the peak at $2\theta \sim 65°$ consists of a MgO peak ($2\theta = 66°36'$) combined with an Fe peak from the Fe seed and capping layers ($2\theta = 65°4'$).

roughness of 0.50 ML, i.e., the original roughness. This clearly indicates that the Fe/Ag system undergoes room temperature annealing, so that, even though the 35 day irradiation period causes detectable damage, it is possible to restore the original quality of the multilayers.

III. X-RAY DIFFRACTION

It is important to establish the structure of the multilayers because this can have a significant effect on the magnetic properties of the samples. All multilayers were therefore characterized with XRD in a θ-2θ geometry for both low and high angles using Cu K_α radiation ($\lambda_\alpha = 1.5405$ Å).

The low angle XRD spectra ($0.5° \leqslant 2\theta \leqslant 16°$) are the result of scattering from the chemical modulation of the layers and give information about the interlayer structure. The high angle spectra ($40° \leqslant 2\theta \leqslant 70°$), on the other hand, are the result of a convolution of the diffraction from the multilayer stack and from a single layer of the constituent materials and give information about the intralayer structure.

The peak positions in low and high angle spectra from multilayered structures are given by[23]

$$\sin(\theta) = \frac{n\lambda_\alpha}{2\bar{d}} \pm \frac{m\lambda_\alpha}{2\Lambda}, \tag{1}$$

with $\Lambda = d_A n_A + d_B n_B$ and $\bar{d} = \Lambda/(n_A + n_B)$, d_A, d_B the lattice spacings and n_A, n_B the number of atomic layers for materials A and B, and n and m integers. The low angle peaks are $n = 0$ peaks while the high angle peaks have $n \geqslant 1$. In the case of the Fe/Ag multilayers, the high angle spectra consist of $n = 1$ peaks.

For all multilayers except the (2,10) system, diffraction peaks are present in both the low and the high angle spectra, indicating good multilayer quality. As an example, the low and high angle spectra of the (3,9) multilayer are shown in Fig. 1, presenting clear diffraction peaks. For the (2,10) system on the other hand, no clear multilayer peaks were seen. Presumably, the latter system is so thin that the large out-of-plane lattice mismatch of 42.5% causes enough roughness to impair the multilayer structure. In this case, we assume that the roughness is at least two atomic layers.

Two programs, based on different approaches, were used to analyze the XRD spectra: Superlattice Refinement by XRD (SUPREX)[23] and SLERF.[24]

The program SUPREX uses the statistical parameters in analytical formulas and fits the spectra using the integral over the different values and their probabilities. It can fit both low angle spectra (with a dynamical theory) and high angle spectra (with a kinematical theory).[23] For the Fe/Ag multilayers, only the part of the high angle spectra between the MgO and the Fe peaks was fitted with SUPREX, see Fig. 1.

The program SLERF uses a Monte Carlo simulation to generate XRD spectra, and only the high angle spectra can be simulated. In Fig. 1, the SLERF simulation result is shown for the high angle spectrum. All high angle spectra of the different multilayers were analyzed with both programs yielding identical results.

Table I shows the roughness parameters obtained from the XRD analysis of the different multilayers. The first two columns give the roughness in monolayers for Ag (σ_{Ag}) and Fe (σ_{Fe}) while the third column gives the interface thickness σ_{int} (ML). The parameters $\sigma_{Ag/Fe}$ are due to the fact that, because of steps and island growth, the number of atomic layers for one Ag or Fe layer is not the same in all places and all bilayers. This is described by a Gaussian function around the average value for the thickness of the layers with $\sigma_{Ag/Fe}$ the width of this function. The parameter σ_{int} for a Ag/Fe interface is the width of the region where the concentration of Ag

TABLE I. The roughness for the different samples given in ML. The system indicated with $^{\text{no cap}}$ is the (3,9) system without an Fe capping layer.

	σ_{Ag} (ML)	σ_{Fe} (ML)	σ_{int} (ML)
$[\text{Ag(3 ML)/Fe(9 ML)}]_{20}$	0.35	0.35	0.6
$[\text{Ag(3 ML)/Fe(9 ML)}]_{20}^{\text{no cap}}$	0.35	0.40	0.7
$[\text{Ag(4 ML)/Fe(6 ML)}]_{20}$	0.40	0.43	0.9
$[\text{Ag(3 ML)/Fe(17 ML)}]_{20}$	0.50	0.55	0.7
$[\text{Ag(6 ML)/Fe(9 ML)}]_{20}$	0.50	0.45	1.0
$[\text{Ag(2 ML)/Fe(10 ML)}]_{20}$	>2	...	...

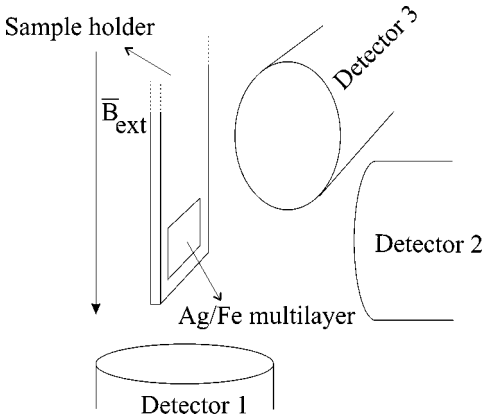

FIG. 2. The LTNO experimental setup with the Ge detectors and the applied magnetic field.

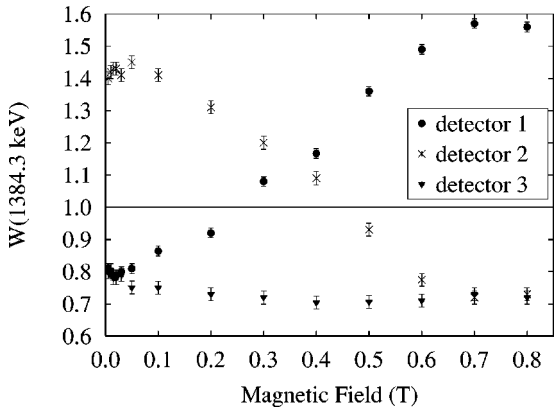

FIG. 3. The γ-ray anisotropy of the 1384 keV γ ray measured as a function of the external magnetic field for the (3,9) system.

drops from 84% to 16% while the Fe concentration increases from 16% to 84%. The concentration is assumed to change following the error function. The (3,9) multilayer without an Fe capping layer has a slightly higher Fe roughness and interface thickness than the (3,9) system with an Fe capping layer. For the (2,10) multilayer no explicit values are given because, as explained above, no peaks were present in the XRD spectra for this system.

IV. LOW TEMPERATURE NUCLEAR ORIENTATION

A. The LTNO measurements

The irradiated multilayers were soldered on to the cold finger of a ^{3}He-^{4}He dilution refrigerator using a Ga—In eutectic with a melting temperature of 25 °C. After inserting the multilayers in the dilution refrigerator, the samples were cooled to temperatures around 6 mK. At these temperatures, the $^{110}Ag^m$ nuclei are oriented, causing the γ rays in their decay to be emitted anisotropically.

The directional distribution of γ rays from oriented nuclei can be expressed as,[25]

$$W(\theta) = 1 + \sum_{k=2,4} B_k U_k A_k Q_k P_k(\cos\theta), \qquad (2)$$

where θ is the angle between the axis of the detector and the magnetic hyperfine field, and $B_k(T, B_{hf})$ are nuclear orientation parameters which depend on both temperature T and magnetic hyperfine field B_{hf}. The U_k and A_k are known nuclear decay scheme parameters, the Q_k are solid angle correction factors and the P_k are the Legendre polynomials.

The directional distribution of the γ rays from the radioactive decay of $^{110}Ag^m$ nuclei in the multilayers was observed with Ge detectors. The experimental setup is shown in Fig. 2. For the measurements of the (3,9), the (3,17), and the (6,9) multilayers, all three detectors were used, while for the other measurements, only detector 1 and detector 2 were utilized.

For all samples, the γ-ray anisotropy was measured as a function of the external magnetic field which was applied in the plane of the multilayers along the Ag(100) axis, see Fig. 2. Because the bcc lattice of the Fe is rotated by 45° with respect to the fcc Ag lattice, this corresponds to the Fe(110) direction. The anisotropy of the 1384 keV γ ray from the decay of $^{110}Ag^m$ as a function of the in-plane applied magnetic field for the (3,9) and the (2,10) multilayers is shown in Figs. 3 and 4. For the other multilayers, a response very similar to that of the (3,9) multilayer was observed.

B. Direction of the Ag hyperfine field

For the 1384 keV γ ray, the parameters B_k, U_k, A_k, and Q_k in Eq. (2) are positive. The Legendre polynomial $P_2(\cos\theta)$ is positive for $\theta \sim 0°$ and negative for $\theta \sim 90°$. Hence, taking into account the fact that the fourth and higher order terms for this γ ray are much smaller than the second order term, a detector a at an angle $\theta \sim 0°$ with respect to the hyperfine field will observe a γ-ray anisotropy $W(\det a) > 1$, while a detector b at an angle $\theta \sim 90°$ will observe a γ-ray anisotropy $W(\det b) < 1$.

All multilayers except the (2,10) system show a LTNO response similar to the one of the (3,9) system shown in Fig. 3. It thus follows that for all multilayers except the (2,10) system, at small in-plane applied magnetic fields, detector 1 is at an angle of almost 90° with respect to the Ag hyperfine field (detailed analysis showed that in fact $75° \leqslant \theta_{\text{det 1}} \leqslant 85°$ for the different multilayers). In addition, in low ex-

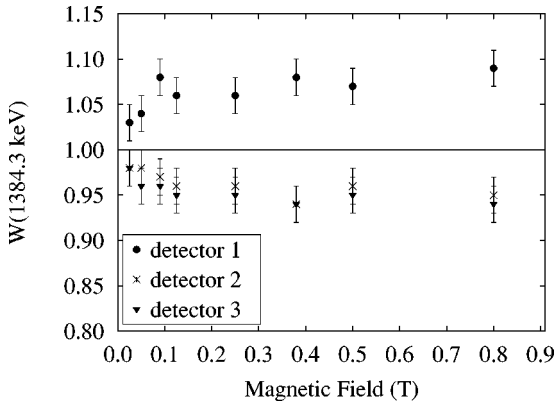

FIG. 4. The γ-ray anisotropy of the 1384 keV γ ray as a function of the external magnetic field for the (2,10) system.

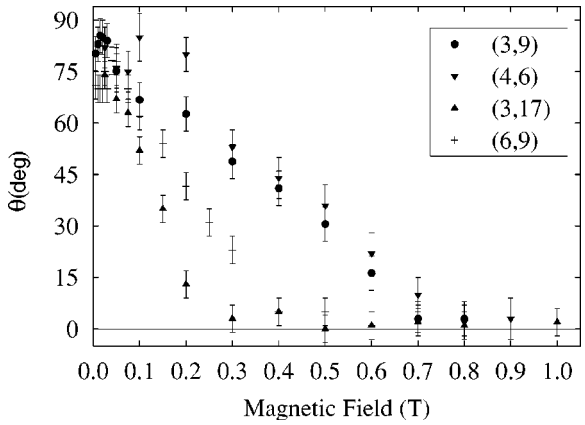

FIG. 5. The angle of the average Ag hyperfine fields with respect to the surface of the multilayers as a function of the applied magnetic field for the different Fe/Ag multilayers.

ternal fields, detector 2 is clearly at an angle of almost 0° ($5° \leqslant \theta_{\text{det }2} \leqslant 15°$). Finally, the third detector, which was used in the measurements of the (3,9), (3,17), and (6,9) samples, is found to be at an angle of almost 90° ($70° < \theta_{\text{det }3} < 80°$) in low applied fields, and fully at 90° for fields higher than about 0.05 T. Thus, taking the respective detector positions into account (Fig. 2), it is clear that the average Ag hyperfine field points out of the plane of the multilayers in zero and low external applied magnetic fields.

For the (2,10) system, which showed no multilayer structure, the observed anisotropies (Fig. 4) clearly show the average Ag hyperfine field to be in the plane of the sample.

The LTNO experiments on the Fe/Ag multilayers further show the Ag hyperfine fields to change orientation as a function of the strength of the external applied magnetic field, as can be seen from the change in γ-ray anisotropy, see Fig. 3. When the external magnetic field is increased, the average Ag hyperfine fields rotate from an out-of-plane to an in-plane orientation. For applied fields larger than the saturation field, the Ag hyperfine fields remain in the plane of the multilayers. From the measured γ-ray anisotropy, the angle of the hyperfine field with respect to the plane of the multilayers can be calculated as a function of the external applied magnetic field. This angle appears to change linearly from the maximum out-of-plane angle Θ_{max} to an in-plane orientation, i.e., $\theta = 0°$, see Fig. 5.

C. LTNO parameters

Several parameters have been derived from the LTNO response to the applied magnetic field. They are summarized in Table II. In the first column, the roughness of the multilayers which was deduced from the XRD measurements is repeated.

The Ag hyperfine field obtained, is listed in the second column. This is the field calculated from the saturation value of the γ-ray anisotropy in high external fields, assuming that only the Ag nuclei at the interface are subject to a magnetic hyperfine field. This assumption is based partially on Mössbauer studies on Fe/Au multilayers,[26] which indicate that the magnetic hyperfine fields in spacer layers are restricted to the interface layer. Moreover, recent PAC measurements on an Fe/Ag interface,[17] show that this is also the case for the Fe/Ag system. The hyperfine fields experienced by Cd probe nuclei at an Fe/Ag interface were measured using PAC. The results showed that only the Cd atoms at the Fe/Ag interface are subject to large hyperfine fields while probe atoms one layer away from the interface in the Ag, experience only a much smaller hyperfine field. Also, first-principles calculations of the magnetic hyperfine fields in Fe/Ag multilayers, to be described in Sec. VI, show that only the interface Ag nuclei experience a significant hyperfine field. Note that the hyperfine field given in Table II is an average of the hyperfine fields at different types of interface sites, i.e., Ag nuclei on flat Fe surfaces as well as Ag nuclei at steps in the Fe layers.

In the third column, the maximum out-of-plane angle Θ_{max} of the hyperfine field with respect to the surface of the samples is given for low applied fields. When the applied field is increased, the angle between the hyperfine field and the sample surface decreases linearly, reaching 0° when the hyperfine fields are in the plane, see Fig. 5. These angles are average angles between the hyperfine field and the direction of the detector since LTNO is not sensitive to the exact distribution of the individual magnetic moments.

The fourth column gives the saturation fields for the different multilayers. This is the value of the external applied field necessary to pull the Ag hyperfine field into the plane of the multilayers.

In the last column, the reduction of the γ-ray anisotropy in low fields is given. From Fig. 3 it can be seen that the maximum γ-ray anisotropy in low field is smaller than the

TABLE II. In this table, the roughness (σ_{Ag}) of the different multilayers is repeated from Table I, and the hyperfine field (B_{hf}) assuming that only the interface Ag nuclei experience a hyperfine field, the maximum out-of-plane angle (Θ_{max}) of this hyperfine field, the saturation field (B_{sat}) and the reduction in γ-ray anisotropy between low and high applied fields (α) are given. The statistical error on the last digit is given between brackets for all values.

	σ_{Ag} (ML)	B_{hf} (T)	Θ_{max} (°)	B_{sat} (T)	α
$[\text{Ag(3 ML)/Fe(9 ML)}]_{20}$	0.35	21.4(8)	85(5)	0.70(5)	0.79(11)
$[\text{Ag(4 ML)/Fe(6 ML)}]_{20}$	0.40	14.9(8)	80(6)	0.80(5)	0.58(12)
$[\text{Ag(3 ML)/Fe(17 ML)}]_{20}$	0.50	11.5(7)	78(5)	0.30(5)	0.38(10)
$[\text{Ag(6 ML)/Fe(9 ML)}]_{20}$	0.50	10.0(6)	74(5)	0.40(5)	0.52(14)
$[\text{Ag(2 ML)/Fe(10 ML)}]_{20}$	>2	3.2(6)	1(5)	0.10(5)	⋯

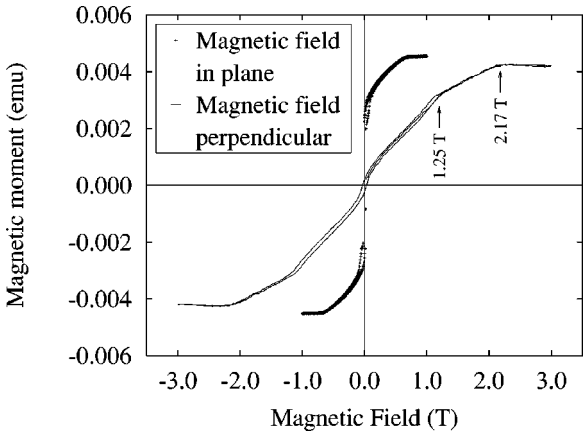

FIG. 6. The magnetization curves obtained at 4 K for the (3,9) multilayer with the magnetic field applied once along the [100] axis of Ag (in plane) and once along the [001] axis (perpendicular). The arrows indicate the multilayer saturation (1.25 T) and the saturation of the Fe seed and capping layers (2.17 T).

saturation value in higher applied fields. This is in part due to the angle of the hyperfine fields with respect to the multilayer plane being smaller than 90° in low applied fields. However, even after correcting for this, the γ-ray anisotropy in low fields is still smaller than that in high fields. The reduction factor α is calculated as, see Fig. 3;

$$\alpha = \frac{(W(\det 2) - 1)_{\text{low field}}}{(W(\det 1) - 1)_{\text{high field}}}, \tag{3}$$

where the low field value is first corrected for the fact that $\theta < 90°$.

A possible explanation for this reduction in γ-ray anisotropy is the fact that the direction of the hyperfine fields experienced by the Ag nuclei would not be the same for all of them. For example, if the Ag moments were lying on a cone, this would result in a smaller γ-ray anisotropy.[27]

V. VIBRATING SAMPLE MAGNETOMETRY

For all multilayers studied here, VSM magnetization curves were measured at different temperatures, ranging from 300 down to 4 K. Measurements were performed with the direction of the applied magnetic field both in-plane (along the [100] axis of Ag, which coincides with the Fe [110] axis and along the Ag [110] axis which coincides with the Fe [100] axis), as well as perpendicular to the plane. Because the values for the saturation field and the remanent magnetization are equal within error bars for the two in-plane directions, the values for the Ag [100] direction are given because this is the direction of the magnetic field during the LTNO measurements. The magnetization curves for the (3,9) system are shown in Fig. 6. For the case when the applied field is perpendicular to the plane, two saturation plateaus are visible (see Fig. 6). The second plateau is found at an external field of 2.17 T for all multilayers. This corresponds to the saturation field for a thick Fe layer (i.e., an Fe layer with negligible surface anisotropy) when a magnetic field is applied perpendicular to the plane. Therefore, this second saturation point is attributed to the Fe seed and capping layers of the multilayers. The first saturation plateau is then interpreted as the actual saturation of the multilayer itself, these fields are listed in the first column of Table III. This interpretation is confirmed by the fact that the VSM measurement of the (3,9) multilayer without the 500 Å Fe capping has only a clear multilayer saturation point. This magnetization curve, at applied fields near the multilayer saturation, reveals characteristic features for a multilayer with an out-of-plane magnetic stripe domain structure,[28] namely a knee in the magnetization curve near saturation with hysteresis. Similar out-of-plane stripe domain characteristics have been found for all the other multilayers except for one sample. The (2,10) system is different from the others: no perpendicular multilayer saturation point was found, only the saturation point at 2.17 T was present (see Fig. 7).

TABLE III. The multilayer saturation fields obtained from the VSM measurements at 4 K for the magnetic field applied perpendicular to the plane ([001] direction) and in the plane (Ag [100] direction). The multilayer marked with $^{\text{no cap}}$ is the (3,9) system without an Fe capping layer. For the (2,10) system, no saturation of the multilayer was observed in the perpendicular configuration (see text).

	B_{sat} (T)	
	Fe [001]	Fe [110]
$[\text{Ag(3 ML)/Fe(9 ML)}]_{20}$	1.25(2)	0.72(4)
$[\text{Ag(3 ML)/Fe(9 ML)}]_{20}^{\text{no cap}}$	1.15(2)	0.61(2)
$[\text{Ag(3 ML)/Fe(17 ML)}]_{20}$	1.61(2)	0.23(7)
$[\text{Ag(6 ML)/Fe(9 ML)}]_{20}$	1.09(9)	0.40(5)
$[\text{Ag(2 ML)/Fe(10 ML)}]_{20}$	⋯	0.10(5)

From the in-plane magnetization curve, a remanent magnetization of 56% is deduced for the (3,9) system, see Fig. 6. For the other multilayers, this value is found to be between 48% and 58%. In contrast, the (2,10) system showed a much

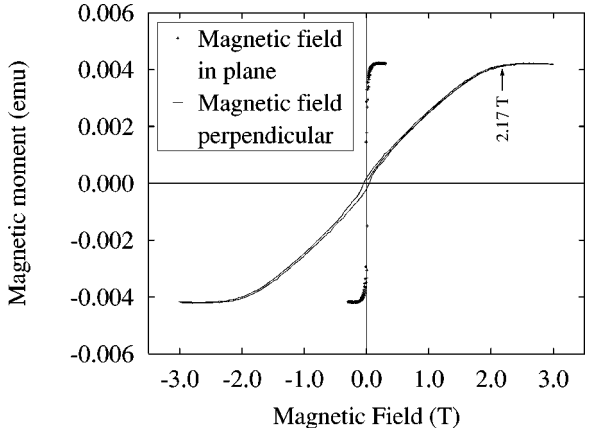

FIG. 7. The magnetization curves obtained at 4 K for the (2,10) multilayer with the magnetic field applied once along the Ag [100] axis (in plane) and once along the [001] axis (perpendicular). The arrow indicates the saturation of the Fe seed and capping layers (2.17 T).

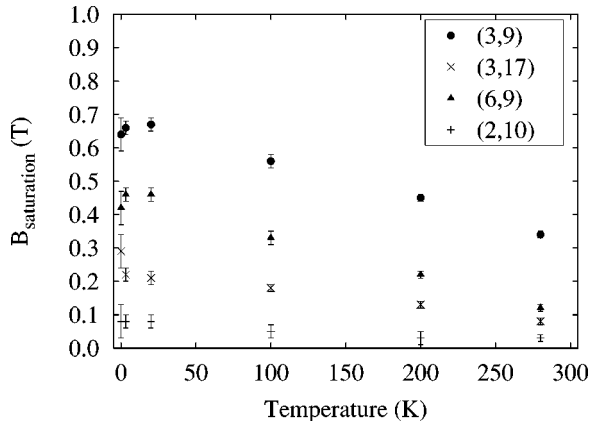

FIG. 8. The in-plane saturation fields for the different multilayer systems as a function of temperature. The lowest temperature point, at 6 mK, is the saturation field measured by LTNO. All other points are measured with VSM. For all multilayers, the saturation fields for the Ag hyperfine field (measured with LTNO at 6 mK) and the Fe magnetization (measured at 4 K with VSM) are equal, within error bars.

larger remanent magnetization of 80%, as seen in Fig. 7. Correspondingly, the observed LTNO signal for this sample found the induced Ag magnetization to lie in the plane, see Fig. 4. Thus the magnetization for the (2,10) sample lies in the plane of the multilayer.

The saturation fields for the external applied field in the plane (Fe [110] direction) of the multilayers at 4 K are listed in the second column of Table III. In Fig. 8, these saturation fields are shown as a function of temperature for the different multilayers. The lowest temperature point for each multilayer is the saturation field as determined from LTNO (taken from Table II, column B_{sat}), the other points are measured with VSM. A comparison of these values shows that the saturation field required to bring the induced Ag hyperfine field into in the plane of the sample is identical (within error bars) to the Fe saturation field for each multilayer. Therefore, the Fe saturation field is the field required to change the magnetic structure of the Fe from out of plane stripe domains to an in-plane orientation. Finally, the effect of the thick 500 Å capping, as demonstrated on the (3,9) sample, was to cause a small reduction in the in-plane and out-of-plane saturation fields.

VI. FIRST PRINCIPLES CALCULATIONS

In addition to the experiments on the multilayers, first principles calculations were performed for different dimensions of Fe/Ag multilayers. For these calculations, the program WIEN97 was used,[29] which was developed to calculate the electronic structure of solids, using the full-potential linearized augmented plane waves method (FLAPW). In our case, the hyperfine fields and the magnetic moments of the atoms in the multilayers were calculated. The multilayer structure is put into a unit cell which is repeated to infinity in all directions. Because the bcc Fe lattice is turned by 45° with respect to the fcc Ag lattice, the unit cell for Fe/Ag multilayers turns out to be quite simple: one atom in every atomic layer is enough to reconstruct the multilayer structure.

TABLE IV. The hyperfine fields and magnetic moments for (1,5) and (3,5) Fe/Ag multilayers calculated with the WIEN97 code. Atoms indicated with (1) are interface atoms, atoms indicated with (2) are atoms one layer away from the interface and so on. The results given are for relaxed atomic positions.

	(1,5)		(3,5)	
	B_{hf} (T)	μ (μ_B)	B_{hf} (T)	μ (μ_B)
Fe(3)	−32	2.5	−31	2.4
Fe(2)	−35	2.3	−35	2.4
Fe(1)	−27	2.7	−28	2.7
Ag(1)	−52	0.05	−32	0.04
Ag(2)	⋯	⋯	−1	−0.001

Calculations were performed for multilayers with different dimensions. Bulk lattice parameters were used to construct the size of the unit cell, while the atomic positions within the unit cell were relaxed, i.e., the atoms were moved to positions where the force acting on them was lower than 1 mRy/Bohr. The results given in Table IV are for the relaxed atomic positions for a (1,5) and a (3,5) system. The calculations did not take into account the spin-orbit coupling nor the dipolar field, the summed contribution of which was calculated to be well below 10% of the values listed in Table IV.

In agreement with the PAC experiment of Ref. 17, only the interface Ag nuclei experience a significant hyperfine field, while Ag nuclei in the second layer away from the interface experience only a very small field. The hyperfine field of −32 T in the Ag interface layer of the (3,5) system was found to be the same for all calculated multilayers with 2 or more monolayers of Ag. It is important to perform the calculations with the atoms at equilibrium positions within the unit cell, since the hyperfine field depends on the Fe-Ag distance. For multilayers with thick Ag layers, the Ag hyperfine fields for the third and fourth layers, were found to be even more reduced: Ag(3) ~ 0.5 T and Ag(4) ~ 0.1 T (results not shown). Only for multilayers with 1 ML of Ag do we find a dramatic change in the Ag magnetic hyperfine field at the interface. For example in the (1,5) system, each Ag atom has eight nearest Fe neighbors, four from each Fe interface, the resulting Ag hyperfine field is −52 T.

The interface Fe hyperfine fields calculated with WIEN97 are lower than the bulk hyperfine field of Fe of −33.728 T.[30] The second layer away from the interface has a higher hyperfine field, but from the third layer on, values close to the bulk hyperfine field are found.

The magnetic moments calculated with WIEN97 for the interface Ag atoms are smaller than the previously predicted value of 0.08 μ_B of Ref. 19 and in agreement with later calculations.[31] For the second Ag layer, the moments turn out to be negligibly small. For the Fe layers, the interface moment is found to be enhanced with respect to the bulk value of 2.2 μ_B in agreement with previous calculations,[19] and with experiments.[32,33]

VII. DISCUSSION

A. Ag hyperfine fields in magnetic saturation

The hyperfine fields listed in Table II are calculated assuming that only the interface Ag atoms experience a magnetic hyperfine field. These values are expected to be independent of the thickness of the layers because all Ag nuclei below the interface are assumed to experience a negligibly small hyperfine field, and consequently, do not contribute to the γ-ray anisotropy. Nevertheless, it is found that the different multilayers have different hyperfine fields, and that the values of these fields are inversely correlated with the roughness of the multilayers, see Table II.

The value of the hyperfine field acting on a Ag nucleus depends on the coordination number, i.e., the number of nearest Fe neighbors, and the distance to those Fe neighbors.[31] The influence of the coordination number is clearly shown by the results of the WIEN97 calculations, see Sec. VI. For the multilayers with thicker Ag layers, all interface Ag atoms are subject to the same hyperfine field of −32 T, caused by the direct *sd* hybridization with the four nearest Fe atoms at the interface. For the multilayer with 1 ML of Ag, the hyperfine field calculated with WIEN97 is higher. In fact, the presence of eight Fe nearest neighbors on both sides of the single Ag monolayer increases the Ag hyperfine field to −52 T. This value is remarkably close to the value of −51 T calculated for a Ag impurity (also with eight nearest Fe neighbors) in a bulk bcc Fe host lattice.[34] The closeness of these two hyperfine fields shows that the number of nearest Fe neighbors is an important factor for the degree of Ag spin polarization. Thus it is clear that roughness should have an influence on the hyperfine field value since this value is strongly influenced by the coordination number and the distance to the Fe nearest neighbors.

When there is a certain amount of roughness present in the multilayers, it follows that the Ag atoms can occupy different possible positions with respect to the Fe surface: on flat terraces, or at a step where the vertical lattice mismatch is 21% causing considerable strain. Thus, the coordination number and the distances to the neighboring Fe atoms are different, leading to lower hyperfine field values. Unfortunately, LTNO cannot resolve the signals from atoms at different locations. Indeed, hyperfine fields measured with LTNO are an average of the hyperfine fields for all different positions. One can therefore conclude that roughness in the multilayers decreases the average hyperfine field experienced by the interface Ag nuclei.

For the (3,9) multilayer with the lowest roughness, the value of the measured interface hyperfine field was found to be $|21|$ T, (see Table II). Since WIEN97 seems to overestimate the Ag hyperfine field (the calculated hyperfine field for a Ag impurity in Fe is −51 T,[34] while the measured value is −44.72(2) T),[35] this value compares rather well with the −32 T calculated with WIEN97 for an ideal surface.

B. Magnetic alignment in Fe/Ag multilayers

For those Ag atoms with nearest Fe neighbors, the small induced Ag magnetic moments are expected to follow the magnetic alignment of those nearest neighbor Fe atoms.[36] Experimentally, collinear alignment was observed also in a PAC measurement on a Fe/Ag bilayer,[17] where the hyperfine fields of the Cd probe atoms in the Ag and the Fe moments were found to be collinear and in plane. The magnetic behavior of the Cd probes is expected to be similar to the behavior of Ag, since the small induced magnetic polarization of the Cd or the Ag *s* electrons is dominated the hybridization with the localized *d* electrons of the Fe.[31,37] Thus we can assume that the observed alignment of the Ag magnetic hyperfine field is equal to the alignment of the Fe nearest neighbors.

Although all studied multilayer systems with well defined x-ray Bragg diffraction peaks have *Q* factors ranging from 0.8 down to 0.28, the Ag hyperfine fields were found to be out-of-plane with average angles ranging from 74° to 85° at 6 mK. From the VSM measurements, these same samples were found to have magnetization curves indicating out of plane stripe domains. However, for the sample (2,10), with no definable diffraction peaks, the induced hyperfine fields of the Ag and the Fe magnetization were found to be in plane.

The influence of roughness on the different parameters can be seen by comparing the multilayers (3,9) and (6,9), with the same Fe thickness (i.e., same *Q* factor), which are expected to have the same K_s and thus the same saturation field. The (3,9) multilayer was found to be smoother, with a corresponding higher average magnetic hyperfine field at the interface (see Table II). This sample also had a larger in-plane B_{sat} (see Table III) indicating a possible increase in the perpendicular surface anisotropy due to a decrease in roughness.[6,7] The corresponding differences were also observed in the alignment of the Ag hyperfine fields at low applied magnetic fields. The Ag fields for the (3,9) sample were found to be almost perpendicular to the multilayer at an average maximum angle of 85(5)° compared to 74(5)° for the (6,9) sample. Comparing samples (3,9) and (3,18) with the same Ag thickness but with different *Q* factors, the (3,18) sample had a lower maximum out-of-plane angle at low applied fields and as expected a smaller in-plane magnetic saturation field. Finally, the reduction of γ-ray anisotropy at low applied fields, measured by α in Table II, also correlates with decreasing roughness.

It is interesting to compare the surprisingly large maximum out-of-plane angles in these samples with angles from other experiments on Fe/Ag multilayers measured by Mössbauer spectroscopy.[38] In this case, a multilayer $[\mathrm{Fe(15\ ML)/Ag(4\ ML)}]_{N=16}$ grown on flat MgO[001] was found to have an average out-of-plane magnetization with an angle of 29°. Another sample, this time grown on a polished MgO[001] with a miscut of 1.8°, was found to have an in-plane magnetization. The spin reorientation observed for the flat substrate was explained to be due to an increase in the perpendicular anisotropy induced by atomic steps. Scanning funneling microscopy (STM) measurements taken after the growing of the first bilayer surprisingly showed that the sample on a flat surface had a higher step density than the sample on the vicinal substrate. It is difficult to compare these results directly with the results from this paper, because of the differences in samples and experimental conditions. In contrast to the multilayers described here, the multilayers in

Ref. 38 have no Fe base and capping layers. Also, the experiments were performed at room temperature, while our measurements were performed at very low temperatures where we can expect increases in the perpendicular surface anisotropy.

In comparison to other out-of-plane magnetization systems, in particular exchange coupled double layer films with one layer with intrinsic in-plane and the other layer with intrinsic perpendicular anisotropy, e.g., Ref. 39), the individual Fe layers in the multilayers studied here, are designed to be in plane ($Q_i 1$), including the base and capping layers. However, the long range coupling effects introduced by the number of bilayers influence the whole sample. It was first observed in Co/Au multilayers that a magnetization reorientation could be induced by increasing the number of bilayers N.[9] Multilayers with Q values ranging from 0.80 to 0.64, were found to have an in-plane magnetization for $N=1,2$, whereas an out-of-plane stripe domain structure was observed for $N=31$. These results were later explained by the theory of Labrune *et al.*,[10] where it was found that a stripe domain structure greatly reduces the demagnetization energy. The key features of this magnetic structure consist of a well defined stripe pattern of up and down domains, as well as a pronounced magnetic domain closure for the top and bottom layers which are magnetized in the plane of the multilayer. Due to the closure of the domains, the stray field energy is considerably reduced. In the middle between the inner up/down domains the domain wall winds around vortices. This theory corresponds very well to the average direction of magnetization observed in the Co/Au multilayers, where the inner Co layers were found to have a larger out-of-plane angle of 54°–60°, than the top and bottom layers of 33°–44°. A possible explanation for the exceedingly large out-of-plane angles observed in our multilayer samples could be the role played by the thick Fe capping and base layers. These layers couple to the multilayer through the long range demagnetization fields and are most likely magnetized in-plane because they have an out of plane saturation point of 2.17 T. Therefore, the base and capping layers could provide a flux closure between perpendicular up and down domains within the thin Fe layers, allowing the Fe layers inside the multilayer structure to rotate freely out of the plane. However, the effect of the capping layers is yet to be determined theoretically.

VIII. CONCLUSIONS

The LTNO results described in this paper provide a unique insight into the magnetic properties of Fe/Ag interfaces, that conventional magnetic methods would find difficult to measure. The method has been shown to have a sensitivity to the structural defects at the interface. Additionally, the long penetration range of the measured γ rays is particularly suited to the measurement of buried interfaces. Especially, in these samples the magnetic structure of the multilayers can be probed separately from the Fe capping layers.

For the multilayers investigated, we have observed that the magnitude of the Ag hyperfine field at the interface correlates with the intra- and interlayer structure studies performed using XRD. The sample with the lowest roughness had a hyperfine field of $|21|$ T. This value can be compared with theoretical studies using the program WIEN97. The WIEN97 calculations also demonstrated that the calculated Ag magnetic hyperfine field is largely dependent on the number of and distance to the Fe nearest neighbors and not the general structure of the system. Furthermore, at low applied magnetic fields Fe/Ag multilayers with Q factors from 0.8 down to 0.28 were found to have out of plane (almost perpendicular) Ag hyperfine fields at millidegrees Kelvin temperatures. The degree of alignment and the average out-of-plane angle at low fields was found to decrease with increasing roughness. VSM studies on these samples confirmed that the magnetic multilayers exhibit a typical out-of-plane stripe domain structure from room temperature down to 4 K. Therefore, the explanation for the almost perpendicular Ag hyperfine fields is the presence of out of plane stripe domains.

ACKNOWLEDGMENTS

The authors are grateful to L. Vanneste for valuable discussions and suggestions, to S. Cottenier for the help and discussions on WIEN97, to J. Dekoster, J. Meersschaut, and the IMBL for the help with the MBE and VSM measurements. M.J.P. would like to thank the Deutsche Forschungsgemeinschaft for generous support.

*Present address: Institut für Experimentalphysik (WE1), Freie Universität Berlin, 14195 Berlin, Germany.

†Present address: SCK-CEN, B-2400 Mol, Belgium.

[1] A. S. Hoagland, IEEE Trans. Magn. **39**, 1871 (2003).

[2] M. L. Néel, J. Phys. Radium **15**, 225 (1954).

[3] H. J. G. Draaisma and W. M. J. de Jonge, J. Appl. Phys. **64**, 3610 (1988).

[4] J. Miltat, in *Applied Magnetism*, edited by R. Gerber, C. D. Wright, and G. Asti (Kluwer Academic, Dordrecht 1992).

[5] K. B. Urquhart, B. Heinrich, J. F. Cochran, A. S. Arrot, and K. Myrtle, J. Appl. Phys. **64**, 5334 (1988).

[6] M. T. Johnson, R. Jungblut, P. J. Kelly, and F. J. A. den Broeder, J. Magn. Magn. Mater. **148**, 118 (1995).

[7] B. Heinrich, Z. Celinski, J. F. Cochran, A. S. Arrott, and K. Myrtle, J. Appl. Phys. **70**, 5769 (1991).

[8] R. K. Kawakami, E. J. Escorcia-Aparicio, and Z. Q. Qiu, Phys. Rev. Lett. **77**, 2570 (1996).

[9] S. Hamada, N. Hosoito, and T. Shinjo, J. Phys. Soc. Jpn. **68**, 1345 (1999).

[10] M. Labrune and A. Thiaville, Eur. Phys. J. B **23**, 17 (2001).

[11] Z. Celinski, B. Heinrich, and J. F. Cochran, J. Appl. Phys. **73**, 5966 (1993).

[12] Z. Celinski, B. Heinrich, and J. F. Cochran, J. Magn. Magn. Mater. **145**, L1 (1995).

[13] J. Unguris, R. J. Celotta, and D. T. Pierce, J. Magn. Magn. Mater. **127**, 205 (1993).
[14] F. A. Volkening, B. T. Jonker, J. J. Krebs, N. C. Koon, and G. A. Prinz, J. Appl. Phys. **63**, 3869 (1988).
[15] D. J. Keavney, M. D. Wieczorek, D. F. Storm, and J. C. Walker, J. Magn. Magn. Mater. **121**, 49 (1993).
[16] R. Meckenstock and J. Pelzl, J. Appl. Phys. **81**, 5259 (1997).
[17] B.-U. Runge, M. Dippel, G. Filleböck, K. Jacobs, U. Kohl, and G. Schatz, Phys. Rev. Lett. **79**, 3054 (1997).
[18] T. Phalet, M. J. Prandolini, W. D. Brewer, P. De Moor, P. Schuurmans, N. Severijns, B. G. Turrell, A. Van Geert, B. Vereecke, and S. Versyck, Phys. Rev. Lett. **86**, 902 (2001).
[19] S. Ohnishi, M. Weinert, and A. J. Freeman, Phys. Rev. B **30**, 36 (1984).
[20] T. Phalet, J. Camps, P. De Moor, P. Schuurmans, N. Severijns, M. Trhlìk, A. Van Geert, L. Vanneste, B. Vereecke, and W. D. Brewer, J. Magn. Magn. Mater. **165**, 234 (1997).
[21] M. J. Prandolini, T. Phalet, W. D. Brewer, J. Dekoster, P. De Moor, N. Severijns, P. Schuurmans, B. G. Turrell, A. Van Geert, L. Vanneste, B. Vereecke, and S. Versyck, J. Magn. Magn. Mater. **198**, 291 (1999).
[22] G. Gladyszewski, K. Temst, R. Schad, F. Beliën, E. Kunnen, G. Verbanck, Y. Bruynseraede, R. Moons, A. Vantomme, S. Blässer, and G. Langouche, Thin Solid Films **366**, 51 (2000).
[23] E. E. Fullerton, I. K. Schuller, H. Vanderstraeten, and Y. Bruynseraede, Phys. Rev. B **45**, 9292 (1992).
[24] G. Gladyszewski, Thin Solid Films **204**, 473 (1991).
[25] K. Krane, in Ref. 40, Chap. 2, p. 31.
[26] Y. Kobayashi, S. Nasu, T. Emoto, and T. Shinjo, in *Conference Proceedings ICAME-95*, 1996, Vol. 50, p. 619.
[27] B. Turrell, in Ref. 40, Chap. 10, p. 475.
[28] J. R. Barnes, S. J. O'Shea, M. E. Welland, J.-Y. Kim, J. E. Evetts, and R. E. Somekh, J. Appl. Phys. **76**, 2974 (1994).
[29] P. Blaha, K. Schwarz, and J. Luitz, Comput. Phys. Commun. **59**, 399 (1990), improved and updated Unix version of the original copyrighted WIEN code.
[30] C. Violet and D. Pipkorn, J. Appl. Phys. **42**, 4339 (1971).
[31] C. O. Rodriguez, M. V. Ganduglia-Pirovano, E. L. Peltzery-Blancá, M. Petersen, and P. Novák, Phys. Rev. B **63**, 184413 (2001).
[32] J. L. Erskine, Phys. Rev. Lett. **45**, 1446 (1980).
[33] A. M. Turner and J. L. Erskine, Phys. Rev. B **30**, 6675 (1984).
[34] S. Cottenier and H. Haas, Phys. Rev. B **62**, 461 (2000).
[35] R. A. Fox, P. D. Johnston, and N. J. Stone, Phys. Lett. **34A**, 211 (1971).
[36] Private discussions with Dr. G. Bihlmayer (Forschungszentrum Jülich): Calculations on Fe/Ag multilayers with noncollinear Fe layer alignment showed that the small induced moment on the Ag atoms at the interface always followed the alignment of the nearest Fe layers. The calculations were performed using the FLAPW mathod in film geometry as implemented in the program FLEUR, see references within Ph. Kurz, G. Bihlmayer, and S. Blügel, J. Appl. Phys. **87**, 6101 (2000).
[37] C. O. Rodriguez, M. V. Ganduglia-Pirovano, E. L. Peltzery-Blancá, and M. Petersen, Phys. Rev. B **64**, 144419 (2001).
[38] B. Degroote, M. Major, J. Meersschaut, J. Dekoster, and G. Langouche, Surf. Sci. **482–485**, 1090 (2001).
[39] R. Sbiaa, H. Le Gall, J. M. Desvignes, and M. El Harfaoui, J. Magn. Magn. Mater. **183**, 247 (1998).
[40] *Low Temperature Nuclear Orientation*, edited by H. Postma and N. Stone (Elsevier Science, New York, 1986).